Kinetics and Mechanism of Substitution Reactions of *cis*-[$PtMe_2(dmso)_2$] with Pyridine

Michael Schmülling and Rudi van Eldik*

Institute for Inorganic Chemistry, University of Erlangen-Nürnberg,
Egerlandstr. 1, D-91058 Erlangen, Germany
Fax: (internat.) +49(0)9131/857387
E-mail: vaneldik@anorganik.chemie.uni-erlangen.de

Received July 4, 1997

Keywords: Platinum substitution / Metal–carbon bonds / *trans*-Labilization / Kinetics / Activation parameters

The substitution reactions of *cis*-[$PtMe_2(dmso)_2$] with pyridine (py) to produce *cis*-[$PtMe_2py_2$] in toluene proceeds in two steps. In the absence of added dimethylsulfoxide (dmso), these steps can not be separated due to the rate constants being very similar. In the presence of added dmso, the rate of the first step, the formation of the monopyridine complex is retarded, which is indicative of a dissociative mechanism. A parallel associative reaction path with pyridine could also be observed. This pathway is independent of the concentration of added dmso. Above a 40-fold excess of dmso, the dissociative pathway is suppressed and only the associative reaction occurs. A plot of k_{obs} vs the pyridine concentration for this pathway is linear at low [py], but shows a saturation at high [py]. This suggests that the reaction occurs via the formation of a precursor-complex, for which the formation constant was found to be 0.32 ± 0.03 M^{-1}. The volume of activation at a high pyridine concentration is −11.4 ± 0.8 cm^3 mol^{-1}, which indicates that the ligand interchange process is of the associative type. The second step, the formation of the bispyridine complex, can clearly be separated from the first reaction step. This step occurs via a dissociative mechanism, as demonstrated by the decrease in k_{obs} with increasing pyridine concentration. The dissociation of dmso was characterized by a rate constant of $(8.1 \pm 0.9) \cdot 10^{-4}$ s^{-1} at 25 °C, $\Delta H^{\neq}$ = 116 ± 9 kJ mol^{-1} and $\Delta S^{\neq}$ = 86 ± 29 J K^{-1} mol^{-1}. At higher pyridine concentrations evidence for a parallel associative reaction was found, for which the rate constant is $(1.3 \pm 0.2) \cdot 10^{-3}$ M^{-1} s^{-1} at 25 °C. The results are discussed in reference to available literature data.

Introduction

Complexes of the type *cis*-[PtR_2S_2], with R = Me, Ph and S = dmso, thioether, have been synthesized and their substitution reactions have been studied kinetically in the past.[1][2][3][4] Mostly bidendate ligands such as bipyridine were used as nucleophiles. Several indications for a dissociative substitution mechanism were found. Plots of the observed rate constant k_{obs} vs the entering nucleophile concentration were curved and showed a dependence on the concentration of the leaving group. The saturation rate constant corresponded to the solvent-exchange rate constant. The complexes showed similar kinetic behaviour and identical saturation values for incoming ligands of different nucleophilicity.[2][4] The activation parameters varied in the range from 64 to 101 kJ mol^{-1} for $\Delta H^{\neq}$ and from −67 to +42 J K^{-1} mol^{-1} for $\Delta S^{\neq}$. Convincing evidence came from the measurement of the volume of activation for solvent-exchange on *cis*-[$PtPh_2(Me_2S)_2$], *cis*-[$PtPh_2(dmso)_2$], and *cis*-[$PtMe_2(dmso)_2$], which was found to be +4.7, +5.5, and +4.9 cm^3 mol^{-1}, respectively.[5] Up to then a dissociative mechanism for Pt^{II} had only been suggested for isomerization reactions, since substitution reactions had always been found to follow an associative mechanism.[6][7] The investigated complexes contained two metal–carbon bonds in the *cis*-position. Carbon is a strong σ-donor and therefore labilizes the *trans*-position during substitution reactions.[8][9] This ground-state labilization, combined with an increased electron density on the metal center, were considered to be the reason for the dissociative mechanism.[4] However, theoretical calculations using the Extended Huckel Theory and ab initio calculations of Molecular Energy Potentials supporting these arguments do not exclude an associative mechanism.[4] A parallel associative reaction path was indeed observed for the investigated substitution reactions; high nucleophile concentrations resulted in deviations from saturation kinetics, and with strong nucleophiles such as bis(diphenylphosphino)ethene only a linear concentration dependence was found.

The mentioned investigations leave several questions unanswered since almost exclusively only substitution reactions with bidentate ligands were investigated. No information was gained concerning the substitution mechanism of the second labile ligand. We have therefore investigated the substitution behaviour of *cis*-[$PtMe_2(dmso)_2$] with pyridine as a typical monodentate ligand in order to distinguish between the two subsequent displacement reactions of dmso. The reactions were studied in toluene as solvent, which allowed a systematic variation of the dmso concentration, i.e. the leaving group. Finally, under some limiting conditions the pressure dependence of these reactions could be studied in order to clarify the nature of the underlying reaction mechanism.

  0009–2940/97/1212–1791 S 17.50+.50/0

Figure 1. UV-Vis spectra for the reaction of *cis*-[$PtMe_2(dmso)_2$] with pyridine; exp. conditions: [Pt] = $5 \cdot 10^{-4}$ M, [dmso] = 0.02 M, [py] = 0.04 M, T = 25 °C, Δt = 20 s

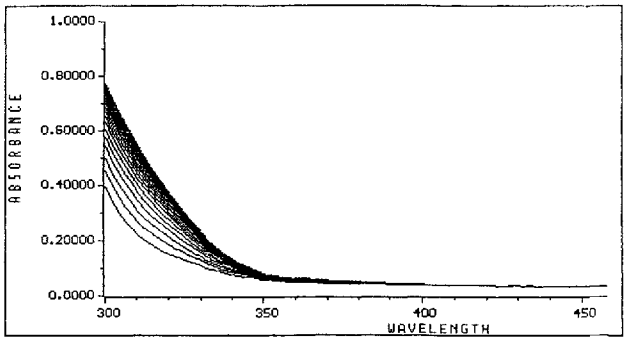

Figure 2a. UV-Vis spectra for the reaction of *cis*-[$PtMe_2(dmso)_2$] with pyridine; exp. conditions: [Pt] = $5 \cdot 10^{-4}$ M, [dmso] = 0.02 M, [py] = 0.1 M, T = 25 °C, Δt = 10 s

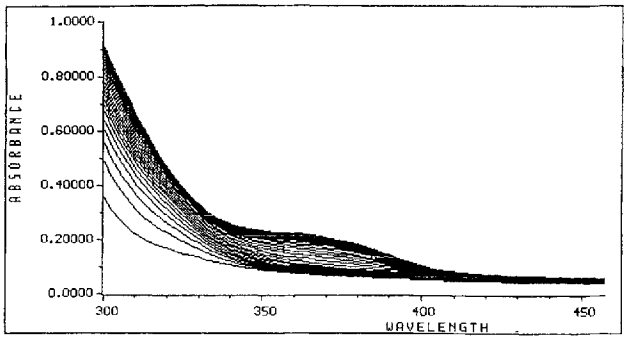

Figure 2b. UV-Vis spectra for the reaction of *cis*-[$PtMe_2(dmso)_2$] with pyridine; exp. conditions: [Pt] = $5 \cdot 10^{-4}$ M, [dmso] = 0.02 M, [py] = 0.75 M, T = 25 °C, Δt = 5 s

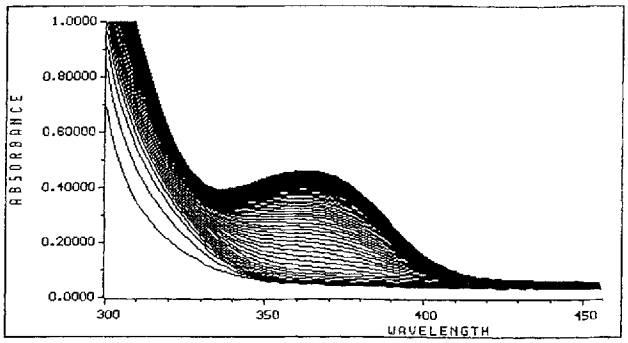

Results

Spectrophotometric Observations

The complex concentration used in all experiments was $5 \cdot 10^{-4}$ M with toluene as solvent. Toluene itself absorbs below 300 nm covering the spectrum of the complex. The observed spectral changes depend on the concentration of both pyridine and added dmso. Reactions at low [py] in a 40-fold excess of dmso compared to the complex concentration, resulted in the formation of a shoulder in the range of 300–330 nm as shown in Figure 1. These spectral changes were assigned to the formation of the monopyridine complex. At higher [py], an additional absorption band at 360 nm appeared following an induction period (Figures 2a and b). An analysis of the absorption-time curves obtained from the recorded spectra at different wavelengths, showed that the band at 360 nm appears only after the formation of the mono- substituted complex is nearly complete. A similar band is reported in the literature for reactions with bipyridine.[2] This band can be ascribed to the formation of the bispyridine complex. At lower concentrations of added dmso, the formation of the bispyridine complex (Figure 3) is significantly faster, such that the two reactions can then not be separated from the observed spectral changes. The rate constants for both reactions are too similar under such conditions that a two-exponential fit of the absorption-time trace at [dmso] $\leq$ 0.005 M does not give reliable results. Therefore a kinetic separation of the two reactions was not possible at low [dmso].

Figure 3. UV-Vis spectra for the reaction of *cis*-[$PtMe_2(dmso)_2$] with pyridine; exp. conditions: [Pt] = $5 \cdot 10^{-4}$ M, [dmso] = 0.005 M, [py] = 0.2 M, T = 25 °C, Δt = 5 s

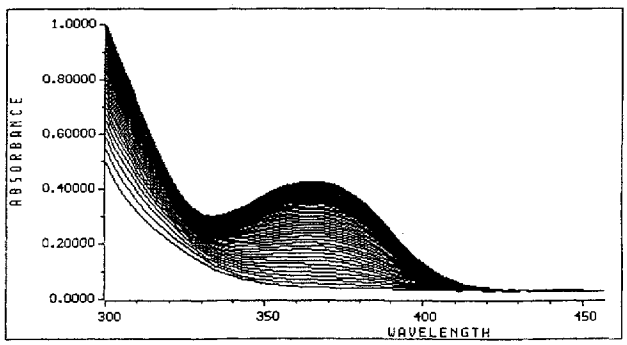

Formation of the Monopyridine Complex

The first reaction, the formation of the monopyridine complex, was studied at different concentrations of added dmso and py. Figure 4 shows a plot of k_{obs} vs concentration of added dmso at different [py]. The observed rate constant decreases with increasing [dmso] and becomes nearly constant above a concentration of 0.02 M. The observed rate constant increases with increasing [py]. This type of kinetic behaviour has also been found for other systems[13], and can be accounted for in terms of the mechanism shown in Scheme 1. Release of dmso leads to the formation of the three-coordinate species, which reacts with pyridine to form the monosubstituted complex. In a parallel reaction path, a direct attack by py occurs, which also leads to the formation of the monosubstituted complex. With increasing concentration of added dmso, the equilibrium is shifted to the left and the direct attack by py dominates. This means that above a certain concentration of dmso the k_1 path is suppressed and only the k_3 path is observed. As shown in Figure 4, the observed rate constant for [dmso] $\geq$ 0.02 M, i.e. at least a 40-fold excess of dmso over the complex concentration, is nearly independent of the concentration of added dmso. Separation of the formation of the mono- and bispyridine complexes at low [dmso] is difficult since the rate constants for these reactions are very similar. The rate con-

Figure 4. Plot of k_{obs} vs the concentration of added dmso at different pyridine concentrations (x = 0.01; o = 0.015; ◇ = 0.02; + = 0.025 M), [Pt] = $5 \cdot 10^{-4}$ M, T = 25 °C, λ = 300 nm

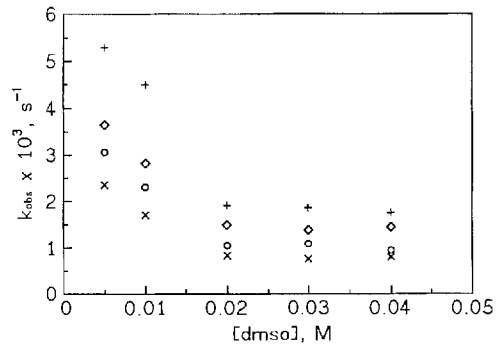

stants reported in Figure 4 for [dmso] = 0.005 und 0.01 M are subjected to large error limits and can only be used to illustrate a trend.

An unexpected dependence of the observed rate constant on [py] was observed at high [dmso]. Figures 5a and b show the corresponding plots and the rate constants are summarized in Table 1. At low [py] a linear dependence is found (Figure 5a), but at high [py] a clear curvature can be observed (Figure 5b). This curvature could be due to medium effects since the pyridine concentrations employed are rather high and an indirect solvent effect is possible. However, the temperature dependence of this reaction, which will be discussed in detail later on, shows even at low [py] a deviation from linearity at higher temperatures. It can also be seen from Figures 5a and b that k_{obs} is independent of the concentration of added dmso and a parallel reaction path is indeed observed. The curvature at high concentrations of pyridine can be explained on the basis of the formation of a precursor-complex along the k_3 path, as it is shown in Scheme 2. The rate law corresponding to this reaction scheme is given in Eq. 1.

Table 1. Observed rate constants for the reaction[a]

cis-[$PtMe_2(dmso)_2$] + py $\xrightarrow{k_3}$ *cis*-[$PtMe_2(dmso)py$] + dmso

[py], M	$k_{obs} \cdot 10^3$, s^{-1} [dmso] = 0.02 M	$k_{obs} \cdot 10^3$, s^{-1} [dmso] = 0.03 M	$k_{obs} \cdot 10^3$, s^{-1} [dmso] = 0.04 M
0.010	0.83 ± 0.09	0.76 ± 0.05	0.80 ± 0.08
0.015	1.05 ± 0.12	1.08 ± 0.06	0.94 ± 0.09
0.020	1.49 ± 0.07	1.38 ± 0.1	1.44 ± 0.09
0.025	1.91 ± 0.13	1.85 ± 0.07	1.74 ± 0.10
0.0375	2.7 ± 0.2	2.9 ± 0.4	
0.05	3.5 ± 0.2	4.0 ± 0.3	3.9 ± 0.3
0.075	6.7 ± 0.3		
0.1	9.3 ± 0.5	9.2 ± 0.6	8.4 ± 0.3
0.125	10.8 ± 0.4		
0.15		12.1 ± 1.0	10.5 ± 0.9
0.175	11.5 ± 0.5		
0.25	17.6 ± 0.6	18.2 ± 1.1	15.9 ± 1.1
0.375	24.5 ± 0.8	24.5 ± 1.7	24.5 ± 1.1
0.5	30.8 ± 0.7	31.0 ± 1.1	31.0 ± 1.4
0.75	42.6 ± 1.0	46.7 ± 1.8	44.3 ± 1.3
1.0	55.5 ± 1.4	57.8 ± 1.7	55.7 ± 2.1
1.25	65.3 ± 1.7	67.3 ± 2.2	67.8 ± 1.9
1.5	74.4 ± 2.3	76.5 ± 2.7	73.3 ± 2.4

[a] Exp. conditions: [Pt] = $5 \cdot 10^{-4}$ M, T = 25°C, λ = 300 nm.

Figure 5a. Plot of k_{obs} vs the pyridine concentration; exp. conditions: [Pt] = $5 \cdot 10^{-4}$ M, T = 25 °C, λ = 300 nm, (o = 0.02; x = 0.03; ◇ = 0.04 M dmso)

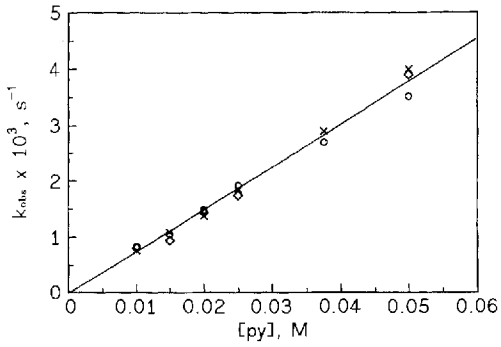

Figure 5b. Plot of k_{obs} vs [py] at high [py], exp. conditions: see Figure 5a

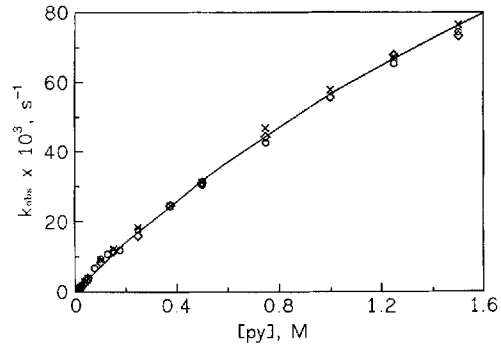

$$k_{obs} = \frac{k\,K[py]}{1 + K[py]} \quad (1)$$

A non-linear fit of the data according to rate law (1) resulted in k = 0.23 ± 0.02 s^{-1} and K = 0.32 ± 0.03 M^{-1}, the equilibrium constant for precursor formation. The rate constant k_3 can be determined from the initial slope of the plot of k_{obs} vs [py], and a value of $(7.6 \pm 0.1) \cdot 10^{-2}$ M^{-1} s^{-1} was calculated. The small value of K indicates that very high concentrations of pyridine have to be employed in order to reach a saturation of k_{obs} (Figure 5b).

Formation of the Bispyridine Complex

The second reaction, the formation of the bispyridine complex, shows a completely different dependence of k_{obs} on [py] and [dmso]. With increasing [dmso], k_{obs} also increases, whereas with increasing [py], k_{obs} decreases and reaches a limiting value. At low [dmso] and high [py], the value of k_{obs} increases again as it can be seen in Figure 6. This type of kinetic behaviour can in general be accounted for in terms of a rate law that involves a linear and an inverse dependence on the entering ligand concentration.[14] The overall reaction scheme is presented in Scheme 3. The monopyridine complex releases dmso, and the three-coordinate species reacts reversibly with py to produce the bispyridine complex. A parallel reaction to produce the bispyridine complex directly, also occurs. The rate law corresponding to this reaction scheme[13] is given in Eq. 2.

Figure 6. Plot of k_{obs} vs the pyridine concentration at different concentrations of added dmso; exp. conditions: [Pt] = $5 \cdot 10^{-4}$ M, λ = 360 nm, T = 25 °C, (o = 0; x = 0.01; ◇ = 0.02; + = 0.03 M dmso)

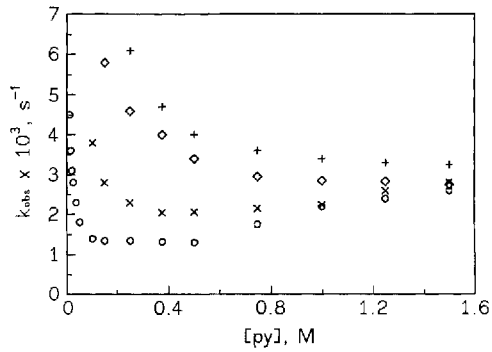

$$k_{obs} = \frac{k_4 k_5[py] + k_{-4}k_{-5}[dmso]}{k_{-4}[dmso] + k_5[py]} + k_6[py] \quad (2)$$

A non-linear fit of the data resulted in rate constants with very large error limits and, depending on the selected iteration conditions, even resulted in negative values. However, the rate law can be simplified depending on the selected conditions. The rate constant k_6 can be calculated from the slope observed at low [dmso] and high [py]. A linear regression treatment resulted in $k_6 = (1.3 \pm 0.2) \cdot 10^{-3}$ M^{-1} s^{-1}. The term k_6[py] can then be subtracted from k_{obs} and this results in Eq. 3.

$$k_{cal} = k_{obs} - k_6[py] = \frac{k_4 k_5[py] + k_{-4}k_{-5}[dmso]}{k_{-4}[dmso] + k_5[py]} \quad (3)$$

An additional simplification turned out to be the assumption that k_5 [py] >> k_{-4} [dmso]. This assumption seems to be plausible, since under the selected conditions the equilibrium should be on the product side, i.e. the bispyridine complex. Therefore Eq. 3 simplifies further to Eq. 4.

$$k_{cal} = k_4 + \frac{k_{-4}k_{-5}[dmso]}{k_5[py]} \quad (4)$$

From Eq. 4 it follows that k_{cal} should exhibit a linear dependence on [dmso] and an inverse dependence on [py]. Plots of k_{cal} versus 1/[py] are indeed linear with a common intercept, and the slopes vary linearly with [dmso]. If k_{-4}[dmso] >> k_5[py] the opposite dependencies should be observed. From a plot of k_{cal} vs the ratio [dmso]/[py] (Figure 7) follows that $k_4 = (8.1 \pm 0.9) \cdot 10^{-4}$ s^{-1}. In this treatment, [dmso] was taken as the sum of the added dmso and that introduced into the system via the *cis*-[$PtMe_2(dmso)_2$] complex, i.e. $1 \cdot 10^{-3}$ M for the data in Table 2.

Table 2 summarizes the observed rate constants k_{obs} and the calculated rate constants k_{cal} in brackets. From Eq. 4 it can be seen that with increasing [dmso], higher pyridine concentrations are required to reach the limiting minimum. Therefore, this minimum is experimentally not observed at the highest applied [dmso]. The slope of the plot of k_{cal} vs [dmso]/[py] represents $k_{-4}k_{-5}/k_5$ and a value of 0.036 ± 0.002 s^{-1} was calculated. Further separation of the rate constants is presently not possible.

Figure 7. Plot of k_{cal} vs [dmso]/[py] following Eq. 4 for the values given in Table 2; (o = 0; x = 0.01; ◇ = 0.02; + = 0.03 M dmso)

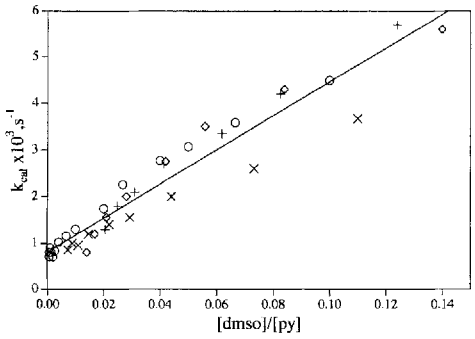

Table 2. Observed and calculated rate constants for the formation of the bispyridine complex[a]

[py], M	$k_{obs} \cdot 10^3$, s^{-1} [dmso] = 0.001 M	$k_{obs} \cdot 10^3$, s^{-1} [dmso] = 0.011 M	$k_{obs} \cdot 10^3$, s^{-1} [dmso] = 0.021 M	$k_{obs} \cdot 10^3$, s^{-1} [dmso] = 0.031 M
0.01	4.5 (4.49) ± 0.3			
0.015	3.6 (3.58) ± 0.3			
0.02	3.1 (3.07) ± 0.2			
0.025	2.8 (2.77) ± 0.2			
0.0375	2.3 (2.25) ± 0.2			
0.05	1.8 (1.74) ± 0.1			
0.1	1.4 (1.3) ± 0.09	3.8 (3.67) ± 0.5		
0.15	1.35 (1.15) ± 0.08	2.8 (2.6) ± 0.1	5.8 (5.6) ± 0.3	
0.25	1.35 (1.02) ± 0.09	2.3 (2.0) ± 0.2	4.6 (4.3) ± 0.5	6.1 (5.7) ± 0.3
0.375	1.32 (0.83) ± 0.06	2.04 (1.55) ± 0.1	4.0 (3.5) ± 0.3	4.7 (4.2) ± 0.5
0.5	1.30 (0.7) ± 0.06	2.06 (1.4) ± 0.12	3.4 (2.75) ± 0.3	4.0 (3.35) ± 0.4
0.75	1.75 (0.8) ± 0.1	2.15 (1.2) ± 0.15	2.95 (2.0) ± 0.2	3.6 (2.7) ± 0.3
1.0	2.2 (0.9) ± 0.1	2.25 (0.95) ± 0.2	2.85 (1.55) ± 0.13	3.4 (2.1) ± 0.3
1.25	2.4 (0.8) ± 0.09	2.6 (1.0) ± 0.2	2.84 (1.2) ± 0.16	3.3 (1.8) ± 0.2
1.5	2.6 (0.7) ± 0.2	2.8 (0.85) ± 0.3	2.75 (0.8) ± 0.12	3.25 (1.3) ± 0.2

[a] Exp. conditions: [Pt] = $5 \cdot 10^{-4}$ M, T = 25°C, λ = 360 nm, [dmso] represents sum of added dmso and that introduced via *cis*-[$PtMe_2(dmso)_2$], i.e. 0.001 M.

Temperature and Pressure Dependences

From the results reported so far the monopyridine complex is formed via two parallel reaction paths according to Scheme 1. The dissociative path is only observed at low [dmso]. Due to the large error limits of the rate constants under these conditions, the activation parameters could not be obtained. At higher [dmso], the parallel k_3 path dominates the formation of the monopyridine complex. Since k_3 is the product of a rate and an equilibrium constant, the activation parameters have to be measured as a function of [py] in order to be able to separate these constants. A temperature dependence study at a high [py] was not possible, since the reaction is then too fast for a normal spectrophotometer and the absorption is too high for our stopped-flow instrument. Figure 8 reports the effect of temperature at low [py]. As mentioned above, at higher temperatures a curved concentration dependence can already be observed at these low concentrations. This indicates that with increasing temperature there is an increase in the precursor formation constant. The rate constant k_3 was calculated from the initial slope, considering only the first few data points at higher temperatures. From the corresponding Eyring plots a value of $\Delta H^{\neq} = 63 \pm 2$ kJ mol^{-1} and $\Delta S^{\neq}$ =

Figure 8. Plot of k_{obs} vs the pyridine concentration at different temperatures; exp. conditions: [Pt] = $5 \cdot 10^{-4}$ M, [dmso] = 0.02 M, λ = 300 nm, (o = 15 °C; x = 25 °C; ◇ = 35 °C; + = 45 °C)

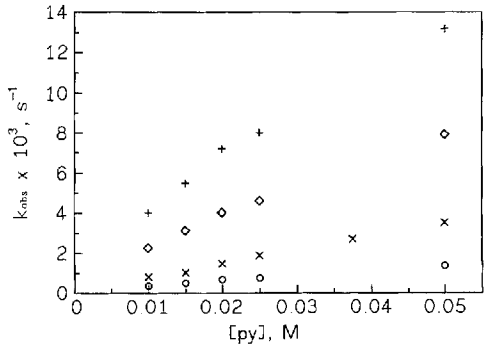

Figure 9. Plot of ln k_{obs} vs pressure for [py] = 0.01 (o) and 0.75 M (x); exp. conditions: [Pt] = $5 \cdot 10^{-4}$ M, [dmso] = 0.02 M, T = 15 °C for [py] = 0.01 M, T = 25 °C for [py] = 0.75 M, λ = 320 nm

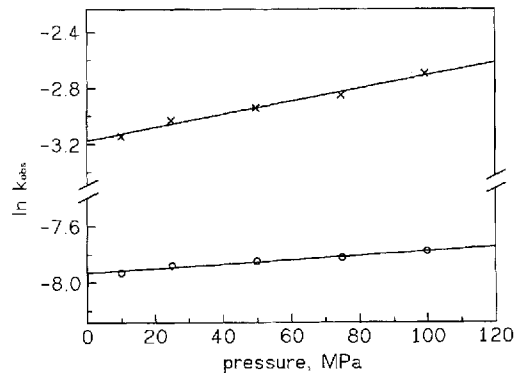

-66 ± 8 J K^{-1} mol^{-1} was calculated. Since k_3 is the product of a rate and an equilibrium constant, it is difficult to draw reliable conclusions concerning the mechanism of the reaction. The negative activation entropy suggests the operation of an associative mechanism.

The pressure dependence of k_{obs} was studied at a low and a high [py]. For experimental reasons the dependence at the low concentration had to be measured at 15 °C. The corresponding plots are shown in Figure 9. A value of $\Delta V^{\neq} = -3.8 \pm 0.5$ cm^3 mol^{-1} for [py] = 0.01 M and $\Delta V^{\neq} = -11.4 \pm 0.8$ cm^3 mol^{-1} for [py] = 0.75 M was calculated.

The influence of temperature on the formation of the bis-pyridine complex was also studied. The corresponding plot is shown in Figure 10. From this plot it can be seen that it is impossible to calculate k_6 at higher temperatures. Therefore k_4 was calculated from a plot of k_{obs} vs [dmso]/[py] from the first three values at 35 and 45 °C. It is reasonable to assume that the influence of the k_6 path in this range is only small, such that at least a maximum value for k_4 can be determined. At 15 °C, $k_6 = (6.9 \pm 0.4) \cdot 10^{-4}$ M^{-1} s^{-1} was calculated from the slope at high [py]. Following eqs. 3 and 4, k_{cal} was calculated and from the corresponding plot $k_4 = (1.3 \pm 0.3) \cdot 10^{-4}$ s^{-1} was determined. The observed rate constants and those calculated from the plot are summarized in Table 3. From the Eyring plot for k_4, $\Delta H^{\neq} = 116 \pm 9$ kJ mol^{-1} and $\Delta S^{\neq} = 86 \pm 29$ J K^{-1} mol^{-1} were calculated. The activation enthalpy is very high, in line with

Figure 10. Plot of k_{obs} vs the pyridine concentration at different temperatures; exp. conditions: [Pt] = $5 \cdot 10^{-4}$ M, [dmso] = 0.01 M, λ = 360 nm, (o = 15 °C; x = 25 °C; ◇ = 35 °C; + = 45 °C)

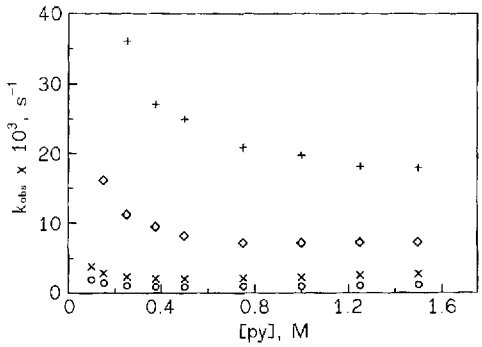

Table 3. Temperature dependence for the formation of the bis-complex[a]

T, °C	[py], M	$k_{obs} \cdot 10^3$, s^{-1}	$k_4 \cdot 10^3$, s^{-1}
15	0.1	1.92 (1.86) ± 0.1	0.13 ± 0.03
	0.15	1.36 (1.27) ± 0.08	
	0.25	1.01 (0.85) ± 0.05	
	0.375	0.85 (0.62) ± 0.06	
	0.5	0.86 (0.55) ± 0.06	
	0.75	0.96 (0.49) ± 0.07	
	1.0	0.98 (0.36) ± 0.1	
	1.25	1.1 (0.23) ± 0.1	
	1.5	1.2 (0.16) ± 0.1	
25	0.10	3.8 ± 0.2	0.8 ± 0.5
	0.15	2.8 ± 0.3	
	0.25	2.3 ± 0.2	
	0.375	2.0 ± 0.1	
	0.50	2.06 ± 0.09	
	0.75	2.15 ± 0.15	
	1.0	2.2 ± 0.2	
	1.25	2.6 ± 0.2	
	1.5	2.8 ± 0.2	
35	0.15	16.2 ± 0,6	4.8 ± 0.6
	0.25	11.3 ± 0.6	
	0.375	9.5 ± 0.4	
	0.50	8.2 ± 0.3	
	0.75	7.2 ± 0.2	
	1.0	7.2 ± 0.2	
	1.25	7.3 ± 0.3	
	1.5	7.3 ± 0.2	
45	0.25	36.1 ± 0.7	12.9 ± 2.7
	0.375	27.1 ± 0.8	
	0.5	25.0 ± 0.7	
	0.75	20.9 ± 0.5	
	1.0	19.8 ± 0.6	
	1.25	18.2 ± 0.7	
	1.5	18.0 ± 0.6	

[a] Exp. conditions: [Pt] = $5 \cdot 10^{-4}$ M, [dmso] = 0.01 M, λ = 360 nm.

that expected for a dissociative reaction. The activation entropy is within the error limits clearly positive.

The pressure dependence of k_{obs} was studied at [py] = 1.0 M and 15 °C, and the results are summarized in Table 4. From the corresponding plot of ln k_{obs} vs pressure, a volume of activation of $+1.9 \pm 0.3$ cm^3 mol^{-1} was calculated. This volume includes the contribution of the k_4-step and the parallel k_6 path. The latter reaction path follows an associative mechanism for which a negative activation

volume can be expected. Therefore, the expected positive volume of activation for the dissociative k_4-step will be partly cancelled, and the actual value of $\Delta V^{\neq}$ for k_4 should be significantly higher. From Table 2 it can be seen that it is impossible to measure k_4 directly, since at every [py] and [dmso], contributions from other reactions are also included. Accordingly, the value obtained from the pressure dependence of k_{obs} represents the minimum volume of activation for k_4.

Table 4. Pressure depence of the rate constant ($k_{obs} = k_4 + k_6[py]$)[a]

p, MPa	$k_{obs} \cdot 10^4$, s^{-1}
10	9.02 ± 0.09
25	8.99 ± 0.07
50	8.90 ± 0.10
75	8.62 ± 0.14
100	8.46 ± 0.17

[a] Exp. conditions: [Pt] = $5 \cdot 10^{-4}$ M, [py] = 1.0 M, [dmso] = 0.02 M, λ = 360 nm.

Discussion

The first kinetic experiments on a platinum complex with two metal–carbon σ-bonds were published in 1984.[1] The solvent-exchange reaction for dmso and substitution reactions of *cis*-[$PtPh_2(dmso)_2$] with bidentate ligands such as bipyridine, 1,10-phenantroline, and 1,2-bis(diphenylphosphino)ethene (dppe), which coordinate via N or P donors, were investigated. For the substitution reactions only one reaction step was observed; the second reaction, i.e. ring-closure, was assumed to be very fast. The kinetic data suggested a reaction mechanism that is in agreement with that in Scheme 1. With increasing concentration of added dmso the values of k_{obs} decreased, which is typical for a competition between dmso and the ligand for a reactive intermediate, a three-coordinate platinum complex. Plots of k_{obs} vs ligand concentration were curved and the double reciprocal plots for different [dmso] showed an intercept independent of and a slope proportional to [dmso]. At high ligand concentrations an additional parallel attack was observed that dominated for dppe with the phosphorus donor atoms.

The investigations were expanded to complexes with σ-bound methyl- instead of phenyl groups and different thioethers as labile ligands.[3][15] In all cases a reaction mechanism involving a direct parallel attack by the entering nucleophile, following Scheme 1, was observed. Evidence for the dissociative nature of the reaction was obtained from the volumes of activation for the solvent-exchange of dmso and thioether for such complexes. Values of +4.7, +5.5, and +4.9 $cm^3\ mol^{-1}$ were measured for the complexes *cis*-[$PtPh_2(Me_2S)_2$], *cis*-[$PtPh_2(dmso)_2$], and *cis*-[$PtMe_2(dmso)_2$], respectively.[5] In addition, the reaction of *cis*-[$PtPh_2(Et_2S)_2$] with pyridine and substituted pyridines was investigated using NMR-methods.[4] All employed pyridines showed saturation kinetics with an identical limiting k_{obs} values, demonstrating that no dependence on the nucleophilicity of the entering ligand existed, which is in line with a dissociative mechanism.

Scheme 1

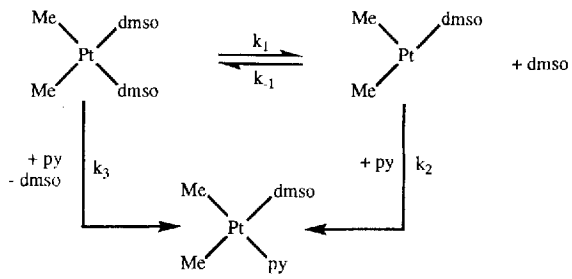

In the present study the substitution reactions of *cis*-[$PtMe_2(dmso)_2$] with pyridine were investigated. It could be shown that it is possible to separate the two subsequent reaction steps kinetically, depending on the ratio of the dmso to the complex concentration. In the absence of added dmso, it is impossible to separate the reaction steps since the rate constants are very similar. With increasing concentration of added dmso, the rate constant for the formation of the monopyridine complex decreases, and higher pyridine concentrations are required for the formation of the bispyridine complex. For a good separation of the two reaction steps, at least a 40-fold excess of dmso over the complex concentration has to be employed. At higher concentration ratios the formation of the monopyridine complex becomes almost independent of [dmso]. The observed dependences on [dmso] and [py] can be accounted for in terms of the reaction scheme given in Scheme 1. As mentioned above, this reaction scheme has also been suggested to apply for reactions with bidentate ligands. The observed mass-law retardation suggests a dissociative reaction step.[13] Further evidence for the dissociative character could not be obtained, mainly because the rate constants at low [dmso] could only be determined with large error limits.

Scheme 2

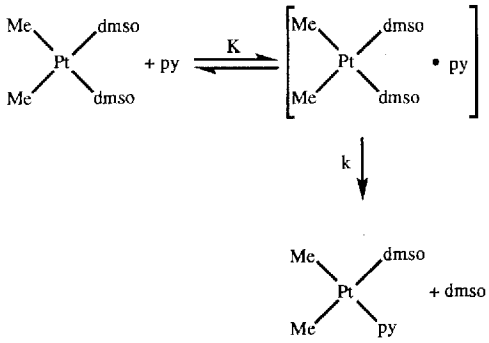

The parallel reaction step occurs via precursor-complex formation as suggested in Scheme 2. The curvature observed in the plots of k_{obs} vs [py] at high concentrations cannot result from the dissociative k_1 step, notwithstanding the fact that saturation kinetics is expected. In that case a dependence on [dmso] must be observed. The lack of this dependence excludes that the k_1 path is investigated. For the k_3 path a rate constant of $(7.6 \pm 0.1) \cdot 10^{-2}\ M^{-1}\ s^{-1}$ was calculated from the initial slope of the data. From the nonlinear fit of k_{obs} vs [py], a precursor formation constant K

of 0.32 ± 0.03 M^{-1} and a limiting rate constant k of 0.23 ± 0.02 s^{-1} for the interchange of the ligands, were calculated. Since k_3 represents the product kK, the activation parameters are also composite quantities. Separation of the different contributions is not always possible. For example, the temperature dependence of the rate constant at higher [py] could not be determined due to experimental difficulties. From the temperature dependence of k_3, calculated from the initial slope of the corresponding plots at low [py], $\Delta H^{\neq} = 63 \pm 2$ kJ mol^{-1} and $\Delta S^{\neq} = -66 \pm 8$ J K^{-1} mol^{-1} were obtained. These values are in agreement with those expected for Pt^{II} substitution reactions.[16] The activation enthalpy is large, but not high enough for a dissociative mechanism. The activation entropy is significantly negative, in line with an associative mechanism for the k_3 path. From the temperature dependence it can only be observed that the curvature in the k_{obs} vs [py] plots starts earlier at higher temperatures, which shows that the pre-equilibrium constant increases with increasing temperature. This observation supports the assumption of a precursor complex formation and contradicts the alternative explanation that the curvature at high [py] is due to secondary medium effects.

A more definite conclusion can be drawn from the volumes of activation determined at low and high [py]. The volume of activation consists of the reaction volume for the precursor-complex formation and the activation volume for the ligand interchange step (Eq. 5). At low [py] the contribution of both is measured, whereas at higher [py] the interchange step dominates.

$$\Delta V^{\neq}(k_{obs}) = \Delta V(K) + \Delta V^{\neq}(k) \quad (5)$$

Due to the small value of the equilibrium constant K, significant saturation could not be observed. Therefore, a separation of $\Delta V(K)$ and $\Delta V^{\neq}(k)$ is not possible. Experimental values of $\Delta V^{\neq}(k_{obs})$ are −3.8 ± 0.5 and −11.4 ± 0.8 cm^3 mol^{-1} at 0.01 and 0.75 M pyridine, respectively. These values clearly support the operation of an I_a or associative mechanism for the parallel k_3 path.

The formation of the bispyridine complex depends, similar to that for the monopyridine complex, on the selected [dmso], as well as the [py]. With increasing concentration of added dmso, higher [py] had to be employed for the complex-formation reaction. With increasing [py] at constant [dmso], k_{obs} decreases after which at very high [py] an increase can again be observed. These dependences can be accounted for by the reaction mechanism shown in Scheme 3.[14] This mechanism essentially corresponds to the one in Scheme 1, the only difference is the equilibrium between the product and the three-coordinate platinum complex. A similar equilibrium for the monocomplex was not observed. In principle such an equilibrium should be possible and should also exist. This equilibrium must be shifted completely to the product side, i.e. the corresponding back reaction is very small.

Interestingly, the bis(dmso) and the monopyridine complexes show different stabilities. The dmso complex dissociatively releases one dmso. At a 40-fold excess of added dmso, the equilibrium is shifted completely to the side of

Scheme 3

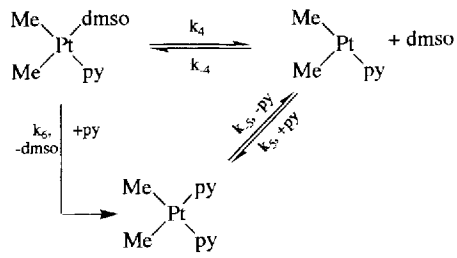

the undissociated complex. The pyridine complex also releases dmso, whereas dissociation of py is not observed. Even at a 60-fold excess of free dmso the release can be observed, which indicates that much higher concentrations are needed to influence the equilibrium. A simple explanation would be that dmso is a substantially poorer nucleophile than pyridine. Alternatively, interaction of π-electrons on pyridine with the vacant p_z-orbital of the platinum center can lead to a less electrophilic platinum center. Such effects are discussed in the literature for the interaction between a benzylamine chelate and platinum.[17]

The only rate constants for the formation of the bispyridine complex that could be determined are k_4 and k_6. k_6 was calculated from the slope of a plot of k_{obs} vs [py] at low [dmso] and high [py] and equals $(1.3 \pm 0.2) \cdot 10^{-3}$ M^{-1} s^{-1} at 25 °C. There are no experimental indications that this reaction path occurs via the formation of a precursor complex analogous to that for the formation of the monopyridine complex. k_4 was calculated from the slope of a plot of k_{cal} vs [dmso]/[py]. A value of $(8.1 \pm 0.5) \cdot 10^{-4}$ s^{-1} was found for k_4 at 25 °C.

For the parallel k_6 path, the temperature dependence could not be resolved, since in the investigated concentration range the increase in k_{obs} could not be observed at higher temperatures. Nevertheless, it can be assumed that this path, as the formation of the monopyridine complex, follows an associative mechanism. The temperature dependence of k_4 supports the dissociative nature of the reaction mechanism. The measured activation enthalpy of 116 ± 9 kJ mol^{-1} is very large and too high for an associative mechanism. A more precise indication is given by the $\Delta S^{\neq}$ value of 86 ± 29 J K^{-1} mol^{-1}, which is clearly positive. From the pressure dependence of k_{obs}, a $\Delta V^{\neq}$ value of +1.9 ± 0.3 cm^3 mol^{-1} was calculated. The volume of activation in this case is the sum of the activation volumes for the dissociation of dmso (k_4) and the parallel k_6 path. If the latter occurs via an associative mechanism, this contribution will be negative. It follows that, as expected for a dissociative reaction step, the volume of activation for k_4 must be clearly positive. The measured value therefore only represents the minimum activation volume.

There are a number of papers dealing with substitution reactions of Pt^{II} complexes containing two metal−carbon σ-bonds in the *cis*-arrangement. As σ-donors C_6H_5, 4-MeC_6H_4, C_6F_5[18], and CH_3 were used, and dmso and different thioethers were the labile leaving groups.[15] For all systems parallel associative and dissociative reaction paths

were observed. The results of the present investigation are in line with these. Unfortunately they cannot offer possible reasons for the changeover in mechanism. Obviously it must be related to the presence of two metal–carbon bonds. One possible explanation could be the strong *trans* effect of the carbon donors. Recently, we investigated the substitution reactions of cyclometallated platinum complexes containing a single Pt–C σ-bond and a water molecule in the *trans*-position.[17][19] Such complexes exhibited the expected high reactivity, but the measured activation parameters corresponded to those normally found for Pt^{II} and Pd^{II} complexes and underlined an associative substitution mechanism.[20]

Table 5. Rate constants for the k_1 path for the reaction of $[Pt(PEt_3)_2RCl]$ with pyridine in ethanol[8]

R	PEt_3 in *cis*-position, R *trans* $k_1 \cdot 10^4$, s^{-1} (T = 25 °C)	PEt_3 in *trans*-position, R *cis* $k_1 \cdot 10^4$, s^{-1} (T = 0 °C)
CH_3	1.7	600
C_6H_5	0.33	380
Cl	0.01	170

The data in Table 5 verify the *trans*- and *cis*-effect of each of the coordinated ligands. On replacing R = Cl in the complex *trans*-$[Pt(PEt_3)_2RCl]$, where Cl is coordinated *trans* to the leaving group, by R = CH_3, k_1 increases by a factor of 170. For the complex *cis*-$[Pt(PEt_3)_2RCl]$, the reactivity is substantially higher, which is only due to the strong *trans* influence of PEt_3. Changing from the now *cis*-coordinated R = Cl to R = CH_3, k_1 increases by a factor of 3. In this example the *trans*-effect is about 50 times stronger than the *cis*-effect, and it is unlikely that such a weak effect can cause the changeover. The reactivity does not seem to play an important role, since Pd^{II} complexes, which are in general by a factor of 10^5–10^6 more reactive, react via an associative mechanism. The complexes $[Pt(CN)_4]^{2-}$ and $[Pt(CNMe)_4]^{2+}$ have also been investigated. For the solvent-exchange reaction very high rate constants (up to 10^5 m^{-1} s^{-1}), and negative volumes of activation were reported.[21] The analogous palladium complexes react only by a factor of 5 and 2 faster, respectively.[21] The ground-state labilization itself cannot play an important role. An X-ray structure of the complex *cis*-$[Pt(Ph)_2(Me_2S)_2]$ has been published.[2] The measured Pt–S distances of 2.37 and 2.389 Å, which belong to the longest known, clearly manifest the labilization. In addition, substitution reactions of the complexes *cis*-$[Pt(Me_2S)_2(Ph)Cl]$, *cis*-$[Pt(Et_2S)_2(Ph)Cl]$, and *cis*-$[Pt(Me_2S)_2(mesityl)Cl]$ with cyanide were investigated.[22] The Pt–Cl distances are 2.409, 2.40, and 2.423 Å, respectively, which are also very long. For these reactions volumes of activation of −6.9 to −16.3 cm^3 mol^{-1} were determined.[22] There is a theoretical study of the reasons for the changeover published in the literature.[4] A combination of ground-state labilization and an increased electron density on the metal center is offered as a possible explanation. An investigation of substitution reactions of *cis*-$[PtPh_2(CO)(SEt_2)]$ with aliphatic amines of comparable basicity and different steric hindrance also supports this.[23] The complex contains three platinum–carbon bonds. For the substitution reactions the well known two-term rate law $k_{obs} = k_1 + k_2[Nu]$, with a clear dependence of the reaction rates on the steric hindrance of the amines and an associative mechanism for the k_2 path, was found. In comparison, a dissociative mechanism was determined for the k_1 path. Carbon monoxide is well known not only for its σ-donor but also for its π-acceptor properties. This means that the electron density at the platinum is affected by CO in a way that is opposite to the complexes with two Pt–C bonds, such that the associative and not anymore the dissociative reaction path dominates. All this shows that we still not fully understand the factors that control the substitution mechanism in square-planar complexes, especially in those cases where metal–carbon bonds affect the lability of Pt^{II} complexes.

The authors gratefully acknowledge financial support from the *Deutsche Forschungsgemeinschaft* and the *Fonds der Chemischen Industrie*.

Experimental Section

Chemicals: The complex *cis*-$[PtMe_2(dmso)_2]$ was prepared as described in the literature and characterized by ^{1}H-NMR and elemental analysis.[10] Chemicals used were of analytical reagent grade and purchased from Merck [pyridine (py) and dimethylsulfoxide (dmso)] and Janssen (toluene). Pyridine and dmso were freshly distilled before use.

Instrumentation: ^{1}H-NMR spectra were recorded on an AM 400 WB Bruker instrument. UV-Vis spectra were recorded on a Varian Cary 1 and an HP 8452 diode-array spectrophotometer. Both instruments could be thermostated to within ±0.1 °C. Kinetic studies were performed in tandem cuvettes, in which the test solutions were thermally equilibrated before mixing. Measurements of fast reactions at elevated pressure (up to 150 MPa) were performed on a high-pressure stopped-flow developed in our group.[11] For slow kinetics at elevated pressure, a high pressure cell[12] built into the cell compartment of the Cary 1 spectrophotometer was used. Both cells were thermostated to within ±0.1 °C. Signal-time curves in the stopped-flow experiments were recorded with an on-line computer. Repetitive-scan spectra of slow reactions were converted into absorption-time curves. For data analysis the OLIS KINFIT (On-Line Instrument Systems, Bogart, USA) set of programs was used.

[1] S. Lanza, D. Minniti, P. Moore, J. Sachindis, R. Romeo, M.L. Tobe, *Inorg. Chem.* **1984**, *23*, 4428.
[2] G. Alibrandi, G. Bruno, S. Lanza, D. Minniti, R. Romeo, M.L. Tobe, *Inorg. Chem.* **1987**, *26*, 185.
[3] D. Minniti, G. Alibrandi, M.L. Tobe, R. Romeo, *Inorg. Chem.* **1987**, *26*, 3956.
[4] R. Romeo, A. Grassi, L.M. Scolaro, *Inorg. Chem.* **1992**, *31*, 4383.
[5] U. Frey, L. Helm, A.E. Merbach, R. Romeo, *J. Am. Chem. Soc.* **1989**, *111*, 8161.
[6] F. Basolo, R. Pearson, *Mechanisms of Inorganic Reactions. A Study of Metal Complexes in Solution*, 2nd ed., J. Wiley & Sons, New York, **1967**, p. 155.
[7] R. Romeo, *Comments Inorg. Chem.* **1990**, 11, pp. 21–57.
[8] M.L. Tobe, *Inorganic Reaction Mechanisms*; Nelson: The Camelot Press Ltd, Southampton, **1972**, p. 58.
[9] R. Demuth, F. Kober, *Grundlagen der Komplexchemie*, 2nd ed., Otto Salle Verlag, Frankfurt am Main, Verlag Sauerländer, Aarau, **1992**, p. 145.
[10] C. Eaborn, K. Kundu, A. Pidcock, *J. Chem. Soc. Dalton Trans.* **1982**, 933.

[11] R. van Eldik, W. Gaede, S. Wieland, J. Kraft, M. Spitzer, D.A. Palmer, *Rev. Sci. Instrum.* **1993**, *64*, 1355.
[12] F.K. Fleischmann, E.G. Gonze, H. Kelm, D.R. Stranks, *Rev. Sci. Instrum.* **1974**, *45*, 1427.
[13] [13a] H.E. Toma, J.M. Malin, E. Giesbrecht, *Inorg. Chem.* **1973**, *12*, 2084. – [13b] J.M. Malin, H.E. Toma, E. Giesbrecht, *J. Chem. Educ.* **1977**, *54*, 385. – [13c] W. Byers, J.A. Cossham, J.O. Edwards, A.T. Gordon, J.G. Jones, E.T.P. Kenny, A. Mahmood, J. McKnight, D.A. Sweigart, G.A. Tondreau, T. Wright, *Inorg. Chem.* **1986**, *25*, 4767. – [13d] K.J. Schneider, R. van Eldik, *Organometallics* **1990**, *9*, 92. – [13e] R.A. Henderson, K.E. Oglieve, *J. Chem. Soc. Chem. Commun.* **1994**, 1961. – [13f] N.E. Brasch, R. van Eldik, *Inorg. Chem.*, in press. – [13g] C. Dücker-Benfer, F.-H. Grevels, R. van Eldik, *Organometallics*, submitted for publication.
[14] J.H. Espenson, *Chemical Kinetics and Reaction Mechanisms*, 2nd Ed., McGraw-Hill, New York, **1995**, p 31.
[15] G. Alibrandi, D. Minniti, L.M. Scolaro, R. Romeo, *Inorg. Chem.* **1989**, *28*, 1939.
[16] R. Romeo, M. Cusumano, *Inorg. Chim. Acta* **1981**, *49*, 167.
[17] M. Schmülling, A.D. Ryabov, R. van Eldik, *J. Chem. Soc. Dalton Trans.* **1994**, 1257.
[18] D. Minniti, *J. Chem. Soc. Dalton Trans.* **1993**, 1343.
[19] M. Schmülling, D.M. Grove, G. van Koten, R. van Eldik, N. Veldman, A.L. Spek, *Organometallics* **1996**, *15*, **1384**.
[20] See e.g. M. Kotowski, R. van Eldik, in *Inorganic High Pressure Chemistry, Kinetics and Mechanisms*, R. van Eldik (Ed); Elsevier, Amsterdam, **1986**, p. 219.
[21] N. Hallinan, V. Besançon, M. Forster, G. Elbaze, Y. Ducommun, A.E. Merbach, *Inorg. Chem.* **1991**, *30*, 1112.
[22] O.F. Wendt, L.I. Elding, presented at the "Inorganic Reaction Mechanism Meeting **1993**" in Wiesbaden, Germany.
[23] R. Romeo, G. Arena, L.M. Scolaro, M.R. Plutino, G. Bruno, F. Nicoló, *Inorg. Chem.* **1994**, *33*, 4029.

[97164]